

ORIGINAL ARTICLE

Fook Choon Choi · Jianchun Li · Bijan Samali  
Keith Crews

## Application of modal-based damage-detection method to locate and evaluate damage in timber beams

Received: September 11, 2006 / Accepted: December 27, 2006 / Published online: April 18, 2007

**Abstract** Modal-based damage-detection algorithms were used to identify the location of defects commonly found in timber and to estimate their severities. In this study, the authors propose modifications to an existing damage-detection algorithm for locating and evaluating damage by comparing the modal strain energy before and after damage using the first two flexural modes of vibration. Experimental verification was performed on pin–pin supported timber beams by employing the algorithms with extracted modal parameters using experimental modal analysis. Single and multiple cases of damage used to simulate pocket(s) of rot with various severities were inflicted by removing sections of timber beam specimens. The proposed damage indicator, computed from the first two flexural modes, was capable of detecting all damage locations. It was also able to estimate, with reasonable accuracy, the severity of damage in term of loss of sectional moment of inertia. The modified damage index method is generally reliable in detecting the location and estimating the severity of simulated defects in timber beams.

**Key words** Damage localization · Severity estimation · Timber · Experimental modal analysis · Modified damage index

### Introduction

Wood is a versatile building material, because it is abundant, easy to obtain, and renewable. It has gained increased interest from engineers over the past decade as a viable material to replace concrete and steel construction.<sup>1</sup> Basi-

cally, wood is a material that is “produced” biologically in the growing tree, making it a nonhomogeneous material that contains growth defects in the form of knots, zones with compression wood, and oblique fiber orientation.<sup>2</sup> This material is also subjected to damage such as termite attacks and pockets of rot as well as mechanical degradation such as overload and fatigue that inevitably weakens its structural capacity and shortens its service life span. Therefore, developing reliable and efficient nondestructive testing (NDT) techniques for evaluation of wood in structures has become a significant task for engineers.

Various local nondestructive testing (NDT) techniques for wood products have been actively developed to provide accurate information on the properties, performance, and condition of wood.<sup>3</sup> However, these techniques are developed mostly to detect faults within a damaged area known a priori, which reduces efficiency and reliability. Thus, global NDT techniques are essential to make the condition assessment of wood more reliable, and time and cost effective. Modal-based damage-detection methods are global NDT techniques that have recently found application in timber structures. However, little research has been reported on timber structures using modal-based methods to detect or to evaluate damage.<sup>4–10</sup> Most of the work to date has been successful in detecting single damage locations and some for two damage locations computed using either the first or second flexural modes.

On the other hand, progress in modal-based damage-detection methods in the laboratory and in the field in recent years has created opportunities for global NDT of timber structures.<sup>4–6</sup> Among various methods, a method developed by Kim and Stubbs<sup>11</sup> based on changes in modal strain energy as a damage indicator for a structure has been particularly promising. In the literature, this method is often referred to as the damage index method. The method was intended for a wide range of applications to structural systems. Recently, published studies have demonstrated the use of the damage index method to localize and estimate the severity of damage within a structure using a limited number of modal parameters for steel plate girder and other highway bridges.

F.C. Choi · J. Li · B. Samali (✉) · K. Crews  
Center for Built Infrastructure Research, Faculty of Engineering,  
University of Technology Sydney, PO Box 123 Broadway, NSW  
2007, Australia  
Tel. +61-2-9514-2023; Fax +61-2-9514-2868  
e-mail: Bijan.Samali@uts.edu.au

This article reports on experimental investigations on timber beams using experimental modal analysis (EMA) to extract the required modal parameters, which are then used to compute the damage index, and hence to detect the damage. A modified damage-detection algorithm was used to locate and evaluate various damage scenarios in the experimental work. A laboratory investigation was conducted on timber beams with damage inflicted under various damage scenarios using modal tests. The modal parameters obtained from the undamaged and damaged state of the test beam were used in the computation of modal strain energy. A statistical approach was also utilized to detect the location of damage. A mode shape reconstruction technique, namely cubic spline interpolation, was used to enhance the capability of the damage-detection algorithm with a limited number of sensors.

## Materials and methods

### Materials

Two timber beams of grade MGP12 were used in the experimental work as undamaged beams with their moisture content estimated to be about 7%–8%. The beams were treated radiata pine sawn timber with nominal dimensions of 45 × 90 mm (width × height) in cross section with a span length of 4500 mm. A specially designed support system was

used to provide a well-defined boundary condition that is very close to a pin–pin support.

### Inflicted damage

The goal of this study was to detect artificial defects in timbers. Both the location of the damage (single and multiple damage) and its severity in timber beams were sought. The cases with various types of damage inflicted in the timber beams are described in Table 1. All damage scenarios consisted of a rectangular opening from the soffit of the beam, located at 1/4, midspan (1/2), and 3/4 of the span length to simulate pockets of rot, which usually starts from the top surface. In this article and the discussions that follow, L, M, and S are used to denote “light,” “medium,” and “severe” damage, respectively. All inflicted damage ( $w$ ) occupied 1% of the total span length (45 mm) and consisted of 10%, 30%, or 50% of the beam depth ( $h$ ), designated as damage cases L, M, and S, respectively, as shown in Table 1 and Fig. 1. The 10%, 30%, and 50% of the beam depth cut in cross section corresponded to losses of sectional “ $I$ ” (moment of inertia) of 27.1%, 65.7%, and 87.5%, respectively.

### Frequency response function

The basic concepts of signal analysis starts with the Fourier transform of a continuous signal, which according to J.B.

**Fig. 1.** Experimental apparatus for modal analysis

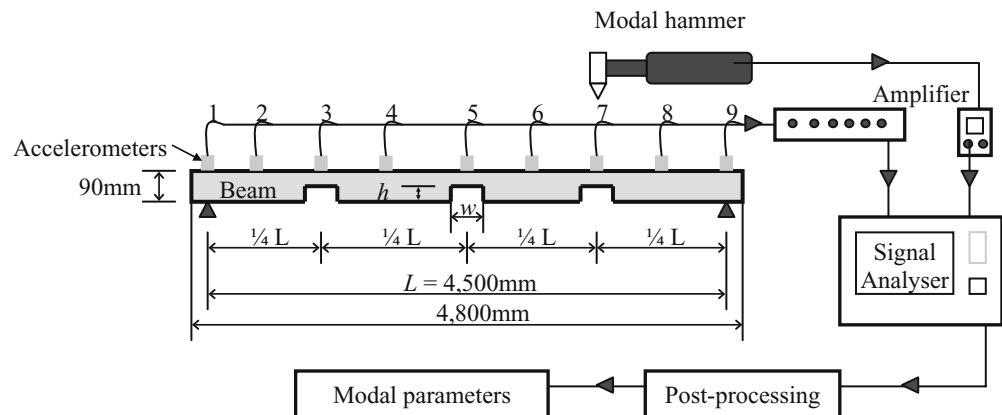


**Table 1.** Inflicted damage scenarios

Damage case	Scenario	Damage location <sup>a</sup>	Width $w$ (mm)	Depth $h$ (mm)	Loss of $I$ (%)
1	4L	4/8 (2.25 m)	45	9	27.1
2	4M	4/8	45	27	65.7
3	4S	4/8	45	45	87.5
4	4S6L	4/8, 6/8 (2.25, 3.375 m)	45	45, 9	87.5, 27.1
5	4S6M	4/8, 6/8	45	45, 27	87.5, 65.7
6	4S6S	4/8, 6/8	45	45, 45	87.5, 87.5
7	2L4L6L	2/8, 4/8, 6/8 (1.125, 2.25, 3.375 m)	45	9, 9, 9	27.1, 27.1, 27.1
8	2M4M6M	2/8, 4/8, 6/8	45	27, 27, 27	65.7, 65.7, 65.7
9	2S4S6S	2/8, 4/8, 6/8	45	45, 45, 45	87.5, 87.5, 87.5

Beam 1 was used for cases 1–6; beam 2 was used for cases 7–9

$I$ , Sectional moment of inertia; L, light damage; M, medium damage; S, severe damage

<sup>a</sup>Given as fraction of span length. Distance from end of beam given in parentheses

Fourier (1822): “any real time signal  $x(t)$  is a superposition of sine waves with their frequency  $f$ , their amplitude  $A$  and phase angle  $\phi$ ”. The fast Fourier transform (FFT) has made it possible to convert time series data to frequency data without losing any information theoretically. In the frequency domain, the input function  $f(\omega)$  with respect to frequency  $\omega$  is obtained from the force applied to the beam with a modal hammer, and the output function  $g(\omega)$  is obtained from the response of the structure measured by the accelerometers attached to the system. By dividing the frequency function of the input by that of the output as shown in Eq. 1, the frequency response function, FRF or  $H(\omega)$  is obtained for each point on the system.

$$H(\omega) = \frac{g(\omega)}{f(\omega)} \quad (1)$$

### Experimental modal analysis

The experimental modal analysis (EMA) procedure and instrumentation layout used for the investigation are shown in Fig. 1. The EMA provides natural frequencies, dampings (not discussed in this article), and corresponding mode shapes. The modal testing, as part of the EMA used in this study, employs an impact hammer to excite the test sample at a strategic location and then the acceleration response is measured. Nine accelerometers were used to measure the acceleration time history of the beam, which was deemed a sufficient number of points along the span so that the mode shapes could be accurately reconstructed using interpolation techniques. One of the accelerometers was used as the driving point measurement, so that the experimental mode shapes could be mass normalized. Each accelerometer was attached using a magnetic base onto a small steel plate that was bolted onto the top of the beams in order to obtain monolithic movement between accelerometer, steel plate, and test beam. The accelerometers were located at 1/8 intervals of the span length starting from one end support of the beam to the other end as shown in Fig. 1. The impact location, at 3/4 of the span length, was selected because it falls on the near-to-peak and peak amplitudes for modes 1 and 2, respectively. Thus, these modes can be excited simultaneously.

A general signal acquisition monitor (HP VXI) was used to record the dynamic response at 10000Hz sampling rate for 8192 data points. A frequency domain direct measurement curve-fitting technique of a postprocessing program (LMS) was used to obtain the modal frequencies and mode shapes from the measured FRFs. Using the EMA, five vibration modes, with a frequency bandwidth ranging from 10 to 200Hz, were captured. However in this article, only the first two flexural modes (see Fig. 2) were needed. From the nine-point experimental mode shape, a new mode shape vector with 41 points could be reconstructed using cubic spline interpolation. The reconstructed mode shape increases reliability and accuracy of damage detection when it is used in damage-detection algorithms.

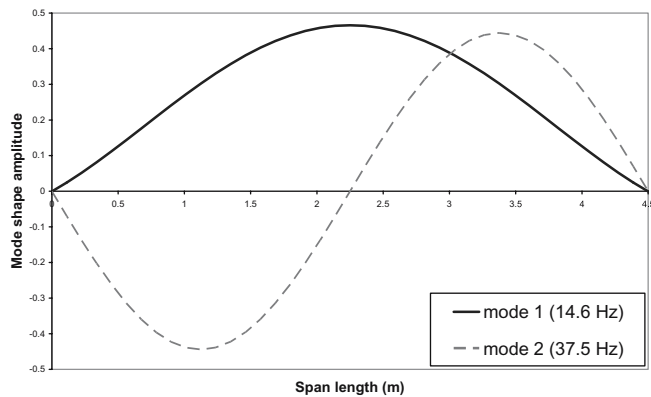


Fig. 2. First two flexural mode shapes

### Damage-detection algorithms

In this investigation, the damage index method developed by Kim and Stubbs<sup>11</sup> was adopted and modified [named as modified damage index (MDI)] to detect the inflicted damage. The MDI pertaining to damage localization is based on the relative differences in modal strain energy between an undamaged structure and that of a damaged structure. The modal strain energy utilizes derivatives of mode shape, that is, mode shape curvature, and the algorithm used to calculate the damage index for the  $j$ th element and the  $i$ th mode,  $\beta_{ij}$ , is given below.

$$\beta_{ij} = \frac{\int_j \{\phi_i^{**}(x)\}^2 dx \int_0^L \{\phi_i''(x)\}^2 dx}{\int_j \{\phi_i''(x)\}^2 dx \int_0^L \{\phi_i^{**}(x)\}^2 dx} \quad (2)$$

In Eq. 2, the terms  $\phi_i''(x)$  or  $\phi_i^{**}(x)$  are normalized mode shape curvature coordinates. The curvature is normalized with respect to the maximum value of the corresponding mode for each mode of a beam structure. This is the major contribution of this article whereby the normalized curvature used in the MDI method is shown to perform better in damage localization than the original formulae (curvature was not normalized).<sup>12</sup> The asterisk denotes the damage cases. For the original damage index method, although mode shape vectors have been mass normalized, the mode shape curvatures used for the damage index calculation are not normalized. Values of mode shape curvature are dependant on the shapes of each individual mode shape. Instead of reflecting the changes in the curvature due to damage, the summation of nonnormalized mode shape curvatures will distort the damage index in favor of higher modes, which results in false damage identifications. The modified damage index method introduced above overcomes the problem by normalizing mode shape curvatures with respect to the maximum norm of each mode shape curvature. To account for all available modes, NM, the damage indicator value for a single element  $j$  is given as:

$$\beta_j = \frac{\sum_{i=1}^{NM} \text{Num}_{ij}}{\sum_{i=1}^{NM} \text{Denom}_{ij}} \quad (3)$$

where  $\text{Num}_{ij}$  is the numerator of  $\beta_{ij}$  and  $\text{Denom}_{ij}$  is the denominator of  $\beta_{ij}$  in Eq. 2. Transforming the damage indicator values into the standard normal space, the normalized damage index  $Z_j$  is obtained:

$$Z_j = \frac{\beta_j - \mu_{\beta_j}}{\sigma_{\beta_j}} \quad (4)$$

where  $\mu_{\beta_j}$  and  $\sigma_{\beta_j}$  are the mean and standard deviation of  $\beta_j$  values for all  $j$  elements, respectively. A judgment based threshold value is selected and used to determine which of the  $j$  elements are possibly damaged, which in real applications is left to the user to define based on the level of confidence required for localization of damage within the structure.

The severity of damage in the  $j$ th member is estimated using the expression as follows:

$$\alpha_j = \left(1 - \frac{1}{\beta_j}\right) \times 100(\%) \quad (5)$$

where  $\alpha_j$  is the severity estimator.

The effectiveness of the modified damage index (MDI) method, introduced above, is closely related to the number of elements of the structure or components. The number of elements to be used by damage detection is dictated by the number of sensors used for the measurement. In order to produce reliable and accurate results, a relatively large number of sensors are required to produce the fine coordinates of the mode shapes. In the numerical simulation, the coordinates can be controlled by mesh density. However, in field applications or experimental testing, the evaluation of the coordinates of the mode shape vectors is limited by the number of sensors used in the test, which is often far less than what the damage detection requires. To overcome this limitation, a few techniques for reconstructing mode shapes to increase the number of coordinates are proposed.<sup>13</sup> In this article, cubic spline interpolation was used for reconstruction of the mode shapes from experimental testing. The measured mode shape coordinates can be interpolated to generate mode shape vectors of greater length.

## Results and discussion

In the following results, all damage localization indices for each of the damage cases are plotted against the beam span length. In principle, any location with the index value  $Z_j$  larger than zero (the probability-based criterion for damage detection) is considered as damage existing at that location. For the estimation of damage severity, the graphs are presented in terms of percentage of loss in “ $I$ ” (sectional

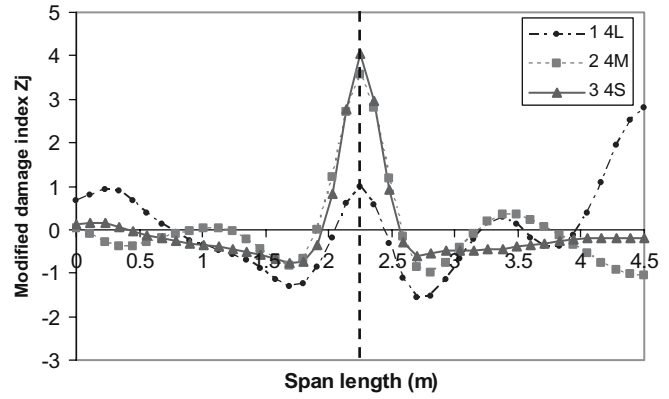


**Fig. 3.** Damage localization for single damage cases 1 to 3. *L*, light damage; *M*, medium damage; *S*, severe damage

moment of inertia). In this case, a weighting coefficient was applied to adjust the severity of damage based on the assumption that the experimental data was polluted with 20%–30% noise (included in the predicted error). The actual damage locations are indicated with dashed lines in all figures.

### Localization of damage

The results of applying the MDI method to compute single damage cases using the first two flexural modes are illustrated in Fig. 3. For single damage cases 1 to 3, the MDI is able to accurately indicate the location of damage at 2.25 m with few false positives (false indication of damage locations) at 3.375 m and near the supports. It is quite clear that as the severity of damage ascends the damage index increases accordingly, having values of 1.00, 3.55, and 4.05 for light, medium, and severe damage, respectively. The noted trend is consistent with the results presented by Hu and Afzal.<sup>9</sup> The damage index is able to qualitatively estimate the location of damage judging from the probability of existence of damage. However, the damage-localization algorithm was not capable of estimating the extent of damage.

Figure 4 depicts the damage scenarios of two damage locations positioned at 2.25 m and 3.375 m detected with MDI. The severe damage for damage cases 4, 5, and 6 was precisely identified by the damage indicator. This also applies to the damage at position 3.375 m except for light damage of damage case 4. It is clear that the method is capable of detecting damage in dual damage scenarios, but may miss light damage that appears together with severe damage. This is due to the light damage slightly altering the mode shape and its derivatives, which may have been overshadowed by other more severe scenarios.

For three damage location scenarios in damage cases 7, 8, and 9, the damage localization results are illustrated in Fig. 5. Again, the MDI method located all damage with a false positive at one of the supports. This has again proven that the method is viable in accurately detecting localized damage for up to three damage locations. However, the damage indicator did not reflect the severity of damage. It

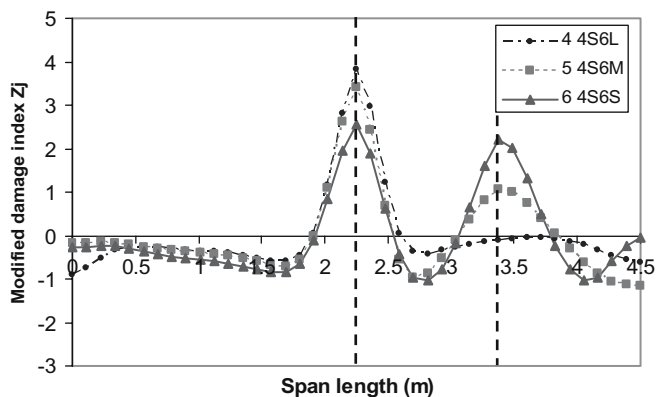


Fig. 4. Damage localization for dual damage cases 4 to 6

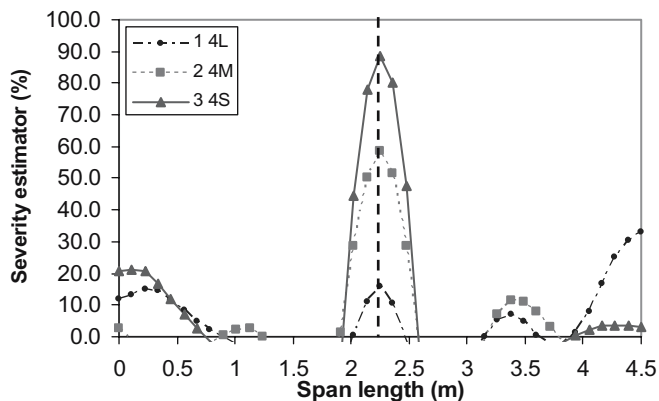


Fig. 6. Severity of damage for single damage cases 1 to 3

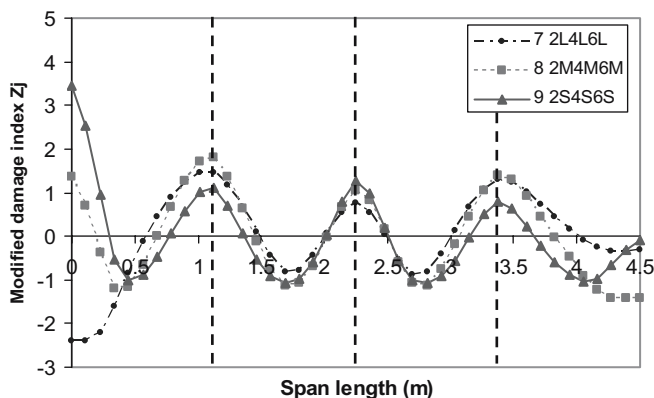


Fig. 5. Damage localization for tri-damage cases 7 to 9

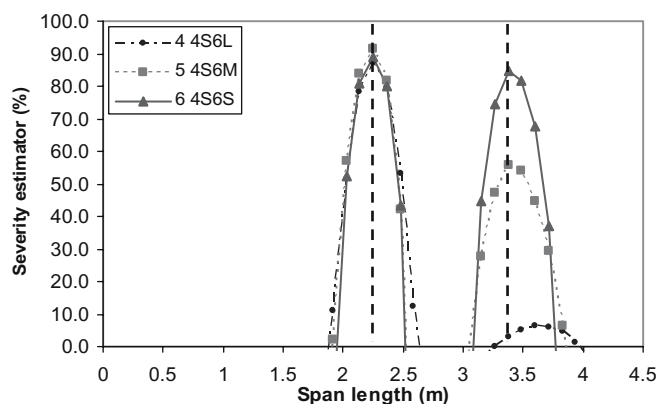


Fig. 7. Severity of damage for dual damage cases 4 to 6

is, therefore, reasonable to conclude that the damage indicator utilizing the statistical approach works well in locating damage but not in evaluating the severity of damage. In light of this, it is important as part of this study to propose a method to evaluate the severity of damage in wood.

#### Estimation of severity of damage

Damage cases discussed above were used in the estimation of severity of damage using Eq. 5. The predicted damage is expressed by loss of “ $I$ ” and it can be directly compared with the simulated damage. The severity of damage below 0% is meaningless; thus, such results are not shown. The results for single damage scenarios at 2.25m are shown in Fig. 6 and the extent of damage is tabulated in Table 2. The damage evaluation algorithm captures the location of damage at position 2.25m very accurately, although there are some false positives. It estimated the severity of damage for severe damage with only 1% error. The prediction of medium-level damage was reasonably good with 11% error. Nevertheless, the error for light damage increased to 40%. The method has shown great potential in estimating severity of damage. It performs well in predicting the extent of

damage from medium to severe for single damage but has reduced accuracy for light damage cases, in addition to its ability to pinpoint the exact location of damage. Any shortcomings of this method can be compensated by other NDT techniques that work well if the damage location is generally known. It is also worth pointing out that in practice, detection of medium or severe damage when it occurs is all that matters in order to avoid catastrophic failure.

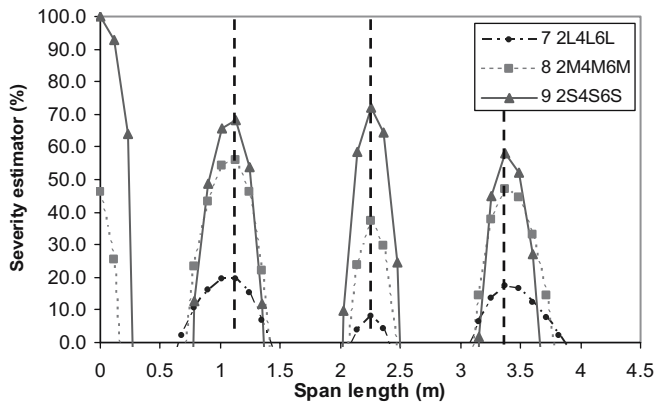
The dual-damage cases 4, 5, and 6 are presented in Fig. 7. The method identified damage at 2.25m and 3.375m. Even the light damage at position 3.375m, which could not be identified using the damage-localization algorithm earlier, was located. From Table 2, the predicted severe damage at 2.25m as well as at 3.375m is fairly accurate with errors of less than 5%; hence, there is high confidence in using the method to evaluate severe damage. For the case of medium damage, the method produced a 15% error in prediction, which still is considered quite acceptable in estimating severity of damage for wood considering the inherent natural variability in wood. However, for light damage, the prediction was relatively poor, although it still showed the location of the damage.

With the success in detecting cases of single and dual damage, it was of interest in this study to explore further

**Table 2.** Estimation of severity of damage for single and multiple damage scenarios

Damage case	Damage location(s) <sup>a</sup>	Simulated damage (%)	Predicted damage (%)	Error (%)
4L	4/8 (2.25 m)	27.1	15.6	42.3
4M	4/8	65.7	58.7	10.7
4S	4/8	87.5	88.6	1.2
4S6L	4/8	87.5, 27.1	87.0, 3.1	0.5, 88.7
4S6M	4/8, 6/8 (2.25, 3.375 m)	87.5, 65.7	91.3, 55.9	4.3, 14.9
4S6S	4/8, 6/8	87.5, 87.5	88.8, 84.5	1.5, 3.4
2L4L6L	2/8, 4/8, 6/8 (1.125, 2.25, 3.375 m)	27.1, 27.1, 27.1	19.7, 8.1, 17.3	27.4, 70.0, 36.2
2M4M6M	2/8, 4/8, 6/8	65.7, 65.7, 65.7	56.0, 37.5, 46.9	14.8, 43.0, 28.6
2S4S6S	2/8, 4/8, 6/8	87.5, 87.5, 87.5	68.1, 72.2, 58.2	22.2, 17.5, 33.4

<sup>a</sup>Given as fraction of span length. Distance from end of beam given in parentheses

**Fig. 8.** Severity of damage for tri-damage cases 7 to 9

the capabilities and limitations of the severity estimation using the proposed algorithm on tri-damage scenarios. These damage cases (7–9) are illustrated in Fig. 8. It is obvious that all damage was detected using the proposed method with a false positive at one of the supports. The error ranges (including the noise level) for light, medium, and severe cases were 30%–90%, 15%–40%, and 20%–35%, respectively. The method could predict the severity of damage reasonably well when three damage locations existed in the structure. It is worth noting that as the number of damage locations increases, the predicted severity becomes smaller than simulated in magnitude. This may be due to the mode shape curvature becoming flat as more damage appears in the test sample. With the insight gained from this study, it is possible to overcome this shortcoming in the future by introducing a sensitivity function of counts and geometric location of damage into the severity estimation algorithm. This initial effort to estimate severity of damage in wood is believed to have advanced the knowledge of NDT for timber structures significantly.

## Conclusions

A modified damage index method was proposed for detecting damage in timber beams using modal parameters obtained from experimental modal analysis. The new

method enhances the existing algorithm in detecting damage location, especially for multiple damage scenarios. It also provides an evaluation of damage severity on timber structures to fill a clear gap in knowledge in this area. The results showed that the proposed algorithm is effective and reliable in locating damage even though it comes with some false positives. The algorithm is also capable of predicting the extent and severity of damage in terms of moment of inertia for single and multiple damage scenarios.

**Acknowledgments** The authors thank the Centre for Built Infrastructure Research (CBIR), Faculty of Engineering, The University of Technology Sydney, for supporting this work. Within the Faculty of Engineering, the authors also thank the staff of the UTS Structures Laboratory for their assistance in conducting the experimental work.

## References

- Moody R (1994) Timber bridges – a rebirth. *Woodland Management* 15(4):18–20
- Thelandersson S, Larsen HJ (2003) *Timber engineering*. Wiley, pp 15–22
- Ross RJ, Pellerin RF (1994) Nondestructive testing for assessing wood members in structures – a review. General Technical Report FPL-GTR-70 (Rev.), Forest Products Laboratory, Department of Agriculture Forest Service, Madison, WI, pp 1–40
- Peterson ST, McLean DI, Symans MD, Pollock DG, Cofer WF, Emerson RN, Fridley KJ (2001) Application of dynamic system identification to timber beam: I. *J Struct Eng* 127:418–425
- Peterson ST, McLean DI, Symans MD, Pollock DG, Cofer WF, Emerson RN, Fridley KJ (2001) Application of dynamic system identification to timber beam: II. *J Struct Eng* 127:426–432
- Peterson ST, McLean DI, Pollock DG (2003) Application of dynamic system identification to timber bridges. *J Struct Eng* 129:116–124
- Yang XY, Ishimaru Y, Iida I, Urakami H (2002) Application of modal analysis by transfer function to non-destructive testing of wood I: determination of localized defects in wood by the shape of the flexural vibration wave. *J Wood Sci* 48:283–288
- Yang XY, Ishimaru Y, Iida I, Urakami H (2002) Application of modal analysis by transfer function to non-destructive testing of wood II: modulus of elasticity evaluation of sections of differing quality in a wooden beam by the curvature of the flexural vibration wave. *J Wood Sci* 49:140–144
- Hu C, Afzal MT (2006) A statistical algorithm for comparing mode shapes of vibration testing before and after damage in timbers. *J Wood Sci* 52:348–352

10. Hu C, Afzal MT (2006) A wavelet analysis-based approach for damage localization in wood beams. *J Wood Sci* 52:456–460
11. Kim J-T, Stubbs N (1995) Model-uncertainty impact and damage-detection accuracy in plate girder. *J Struct Eng* 121:1409–1417
12. Choi FC, Li J, Samali B, Crews K (2006) Damage detection in a timber beam. *Structural Faults and Repair*, 13–15 June, Edinburgh, Scotland, CD-Rom
13. Choi FC, Li J, Samali B, Crews K (2006) Impact of different numerical techniques on damage identification in structures. Tenth

East Asia-Pacific Conference on Structural Engineering and Construction, 3–5 August, Bangkok, Thailand, pp 111–116

---

The publication of this article was made possible by an Emachu Research Fund. The authors are grateful for the fund.